Solder-less Fine Pitch Copper-to-Copper Bonding

Nicholas Lay, Kaysar Rahim, Ph.D.
Northrop Grumman Corporation
7323 Aviation Blvd, Baltimore, MD 21240
Ph: 410-892-2147
Email: Nicholas.Lay@ngc.com, MD.Rahim@ngc.com

Abstract

The industry has been looking to increase pitch scaling through various methods. One of these methods is an alternative to solid-state solder bonding. However, very few processes can compete with solder bonding's fast speed, low cost, and flexibility. The approach with the biggest potential for connecting fine pitch interconnects in high-density semiconductor packaging is solder-less copper-to-copper direct bonding.

There are many benefits to using copper-to-copper direct bonding, including the ability to achieve ultra-fine-pitch (bump pitch 10 μm), higher reliability (both thermo-mechanically and better electromigration behavior), low resistance, as well as the lack of concern for solder hierarchy for multiple reflow. This copper-to-copper direct bonding technology enables a variety of 2.5D/3D advanced packaging architectures and is also suitable for multi-die stacking.

In this study, we report the investigation of a direct copper-to-copper bonding methodology and reliability of the bonded components. Our process differs from common hybrid bonding copper-to-copper techniques, in that it is designed for low volume highly complex products. This technology allows a die-to-die and die-to-wafer process using thermocompression bonding under a deoxidizing vapor flow for direct copper-to-copper bonding. The process does not require high temperature oven annealing and can be done in a normal atmospheric environment. The investigated bonding process is ideal for high power, high thermal, high density 3D stacking and high-speed digital communication applications.

We demonstrated the bonding procedure using a test vehicle with 40 μm diameter pillars and 80-μm bump pitch. We investigated the effects of bonding force and evaluated joint reliability. Interconnect/bond strength was determined through destructive shear testing and cross-sectional analysis. A scanning electron microscope was used to inspect and examine the bonded joint quality. Finally, completed assemblies were thermal cycled to evaluate degradation of joint strength under induced stress, and resistance measurements were performed to evaluate the electrical performance of the bonded copper joint.

Key words

Advanced Packaging, Copper, Die to Die, Direct Bonding, Interconnect, Thermocompression Bonding

I. Introduction

Copper pillars and micro-bumps have been a mainstay interconnect technology for the packaging industry. The most advanced copper pillars or bumps use 40 μm pitch. Next generation packaging architectures can reduce this to 20 μm pitch or 10 μm pitch [1]. Direct bonding (Cu-to-Cu) provides a pathway to tighter pitches and higher density interconnects. Direct bonding has been intensively researched for many years, and serves as a likely substitute for solder joints in advanced packages for fine pitch high density integration, high speed digital communications and higher electrical and thermal performance [2]. Solderless Cu-to-Cu interconnects do not experience degradation phenomena typical of solder interconnects (e.g., intermetallic compounds (IMC)). Bonded copper interconnects can operate at higher temperatures relative to conventional solder bumps because the melting point of the copper is substantially greater than that of the solder [3-4]. Direct bonding of Cu-to-Cu provides several other advantages that are critical to fine pitch assembly for advanced packaging. These advantages include ultra-fine-pitch interconnects (pitch < 10um) that allow for higher reliability, lower resistance, lower RF Loss, higher density, higher speed, higher bandwidth interconnect, and higher thermal budget interconnect. Lastly, the process can be performed repeatedly using the same metallurgy, without need for solder reflow temperature hierarchy. These properties are desirable for 3D die stacking.

In this paper, we report development of a direct Cu-to-Cu bonding process designed for low volume highly complex

products. This process does not require high temperature oven annealing and can be done in normal atmospheric environment via thermocompression bonding while utilizing a deoxidizing gas to allow for direct Cu-to-Cu bonding to occur. This process offers a low cost, reliable method for vertically stacking of components.

We demonstrated the bonding procedure using a test vehicle with 40 µm diameter Cu pads at 80 µm bump pitch. Both dies and interposer pads are plated with 300nm thick silicon oxide and have 7 µm copper pads. We investigated the reliability of copper to copper direct bonded interconnects. Interconnect integrity was assessed through destructive shear testing and cross-sectional analysis to evaluate the bond quality and strength. Test assemblies were subjected to thermal cycling to evaluate joint strength degradation. Electrical resistance measurements were performed on the test pieces to evaluate the electrical performance of the Cu joint.

II. Test Vehicle

A custom daisy chain test vehicle, shown in Fig. 1, was fabricated for bonding process development, consisting of a silicon test die (top) and a corresponding silicon interposer (bottom). The die is 5x5mm, while the interposer is 10x10mm; both silicon parts are full thickness (760 µm). The test assembly features an array of 9 daisy chains to allow electrical resistance and continuity monitoring in different areas of the die. These separate daisy chains were used to identify and locate failure points in the bonded assembly. Each daisy chain was comprised of 400 interconnect with a total of 9 separate chains totaling to 3600 interconnects. Each pad is 40 µm diameter x 7 µm thick plated Cu to allow for the formation of the bonding interface. The pads are 40µm in diameter with 80 µm pitch between each pad.

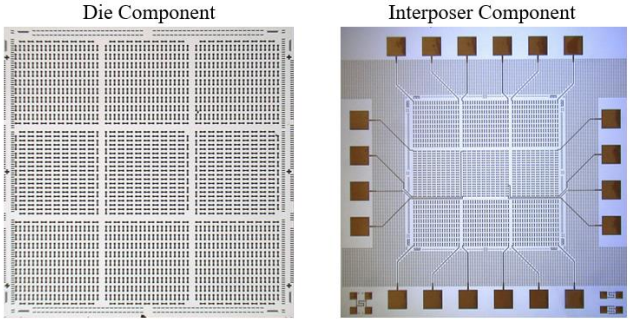

Figure 1: Images of the test vehicle components, including the (a) top die and (b) bottom interposer. The interposer features large pads on the outer perimeter for use in electrical monitoring of each daisy chain.

In addition, we have also included images of our daisy chain structure. In this structure, we have 9 chains on each die monitoring different locations on the die. The 9 chains are independently monitored during temperature cycling. A diagram of the chains and actual interposer design are shown in Fig. 2.

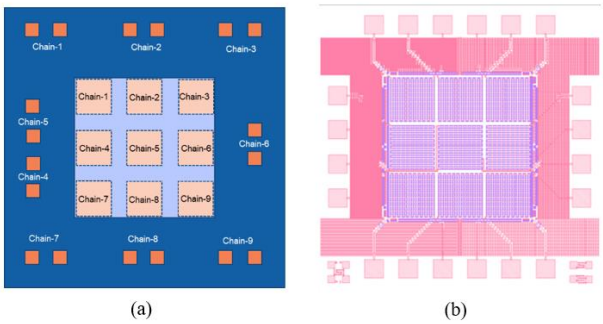

Figure 2: (a) Representation of the daisy chain structure for the test vehicle, and (b) actual design layout of the interposer.

III. Experimental Procedure

Direct Cu-to-Cu bonding was accomplished using a thermocompression (TC) bonding process. Cu bumps are joined without a solder through the application of heat and force while in the presence of formic acid vapor as a chemical reducing agent. Prior to TC bonding, both the die and interposer surfaces were subjected to plasma cleaning to remove organic or other contamination on the Cu surfaces. Formic acid vapor was used as an *in situ* deoxidizing agent during TC bonding. Formic acid vapor was preferred due to better performance in TC bonding when compared to a liquid immersion method [5]. As shown in Fig. 3, the formic acid vapor was created by flowing a nitrogen carrier gas through a formic acid solution, and then passed over the components during TC bonding to allow for a smooth non-oxidized bonding interface.

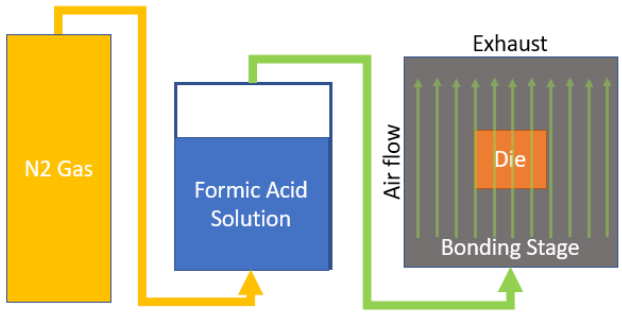

Figure 3: Formic acid application process during TC bonding, involving flowing a N_2 carrier gas through a formic acid solution, which is then passed over the components during bonding.

The formic acid vapor was applied to the die and interposer as a preconditioning step for the Cu surfaces; the vapor flow was continued during TC bonding itself. Then pressure and heat are then added to allow for copper diffusion between the two exposed copper interface forming the interconnection. The bonded assemblies were not

subjected to additional annealing steps and were progressed to mechanical and electrical characterization as-bonded.

The bonded assemblies were subjected to die shear testing to evaluate the Cu-Cu interface quality and mechanical strength. Scanning electron microscopy was used to evaluate cross-sections of the bonded assemblies for bond quality. Electrical and reliability characterization were performed on the bonded assemblies, as described in Section IV.

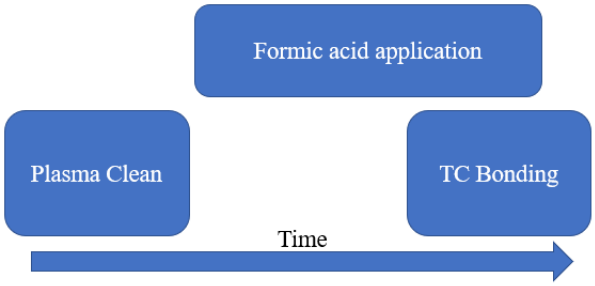

Figure 4: Block diagram representing the process flow for bonding. After plasma cleaning, the formic acid vapor flow is applied both before (preconditioning) and during TC bonding.

IV. Results and Discussion

TC Bonding Process Development

Optimization of the bonding process was required to generate adequate bond strength without the need for a post-bond annealing process. There are three major factors involved in the formation of this interconnect: force, temperature, and formic acid quantity. Here the importance of each is evaluated using the Taguchi Method [6]. The Taguchi Method minimizes the sample size needed to determine the primary factors that affect bond strength, as assessed via die shear testing. In Fig. 5 the effects of force, temperature and formic acid are shown on die shear strength. Samples exhibiting die shear values below the dotted line in Fig. 5 failed optical inspection and did not have acceptable shear force values. The key points and the impact of each factor are summarized below:

1. Copper interface for this trial required a bonding temperature higher than 250ºC for joint formation to occur.
2. Presence of formic acid is critical. Without formic acid bonding will not occur.
3. Increased force increases bond strength.
4. Increased temperature has the greatest effect for increasing bond strength.

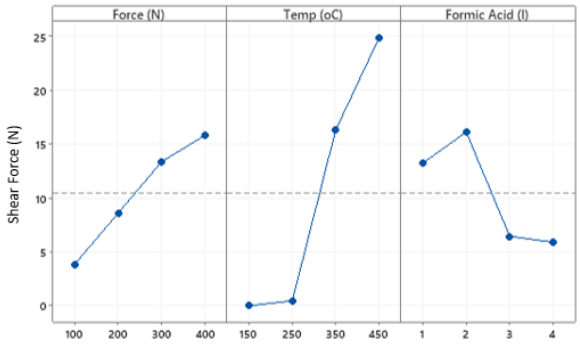

Figure 5: Taguchi method analysis of the effects of TC bonding force, temperature, and formic acid quantity on die shear force to failure.

A design of experiment (DOE) was then conducted to further optimize bonding temperature and force. Table I highlights the DOEs including the corresponding pressures and temperatures. Fig. 6 shows a representative set of the process conditions from the DOE.

Table I: DOE Parameters of Temperature and Bonding Pressure

DOE	Temperature	Pressure
1	325°C	55KgF
2	400°C	500KgF
3	400°C	900KgF

Inadequate bonding conditions (Fig. 6a) yielded interconnects that were under-compressed, with an observable seam between the two components indicating the two parts did not completely bond to each other. In Fig. 6b, slight misalignment was observed, but with no seam between the two die indicating sufficient Cu-to-Cu bonding. In Fig. 6c, with slight over-compression of the die, no seam was seen. However, the goal was to minimize stress on the die to prevent die cracking, so extra high force and temperature was avoided.

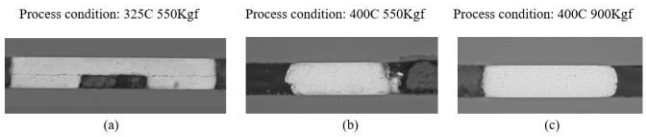

Figure 6: Cross-sectional results of DOE 2 showing (a) incomplete bonding, (b) acceptable bonding, and (c) over-compression that risks potential cracking in the components.

After selecting optimized bonding conditions, assemblies were bonded as shown below in Fig. 7 for further electrical and reliability characterization.

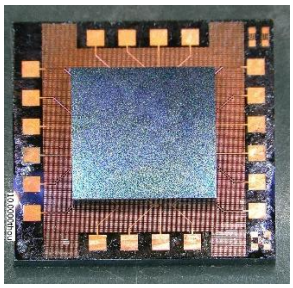

Figure 7: Bonded assembly with die and interposer.

The electrical connectivity of the daisy chain structures (shown previously in Fig. 2) were investigated on these bonded assemblies. Fig. 8 shows the resistance measurement data of sixteen bonded assemblies. None of the chains were shorted (except Chain 3, which shorted on all the dies and was excluded from the data below). All the other chains exhibited low resistance values ranging from 3-5 Ω. Chain 5 (grey), which is the center chain on the die, typically exhibited the lowest resistance indicating likely slightly higher pressure in the center versus the edge of the die.

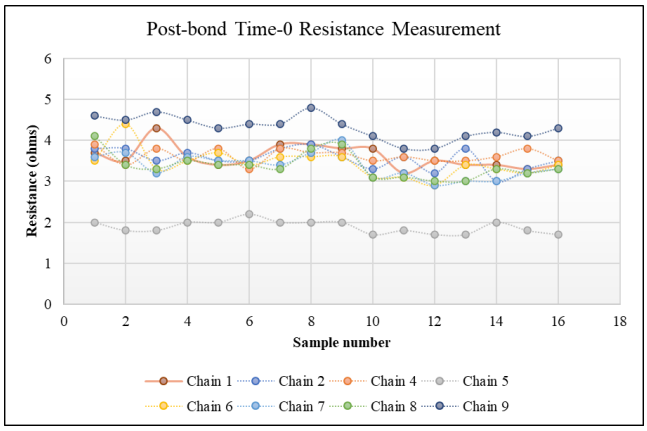

Figure 8: Post-bond time-zero resistance measurements of the daisy chains across 16 different bonded assemblies.

Temperature Cycling

With electrical connectivity verified, the components were temperature cycled. The assemblies were subjected to 1000 cycles of a -55ºC to +125ºC range to check for degradation of the joints through thermal stress. Resistance probing and cross-sectional images were recorded post-cycling. The temperature cycling profile used for this study is shown in Fig. 9, using a 68-minute cycle with a 15-minute stabilization period at +125ºC and a 20-minute stabilization period at -55ºC.

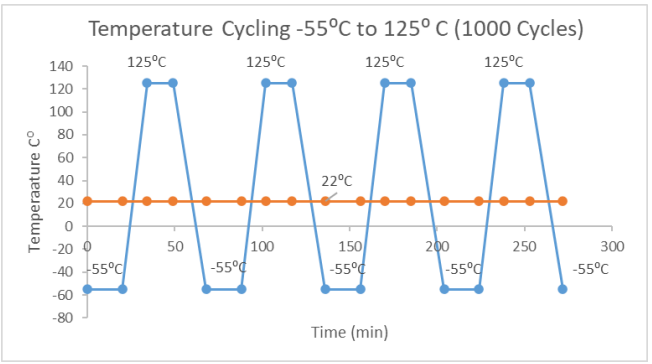

Figure 9: Temperature cycling profile used in bond integrity testing.

We monitored the post-bond daisy chain resistance incrementally, up to 1000 total cycles. Figs. 10 and 11 show the resistance measurements and variations for 16 samples for the corner Chains #7 and #9, respectively, while Fig. 12 shows the resistance variation of the center Chain #5. For all three chains, the data shows a slight increase in resistance through 1000 cycles. However, none of the chains are shorted or opened after completing all cycles.

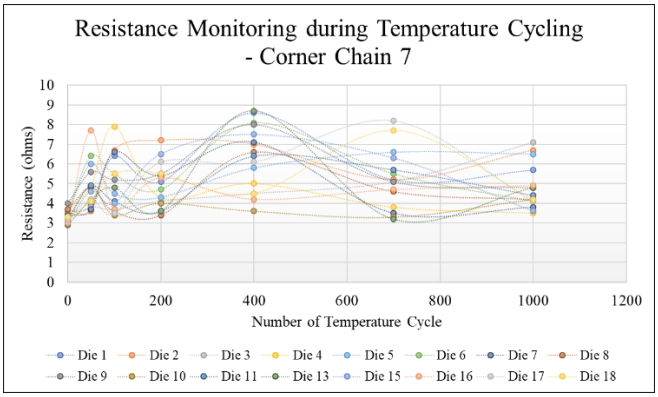

Figure 10: Resistance monitoring through temperature cycling of corner Chain #7.

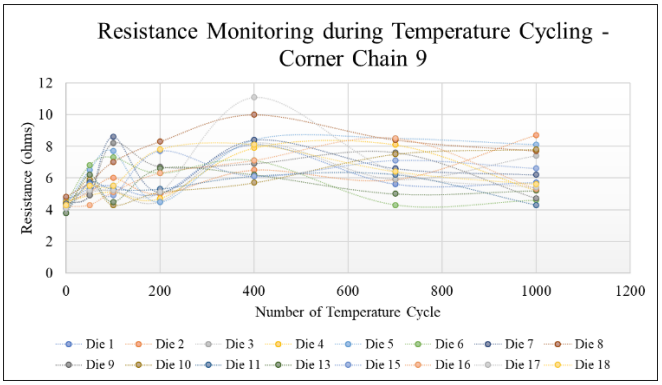

Figure 51: Resistance monitoring through temperature cycling of corner Chain #9.

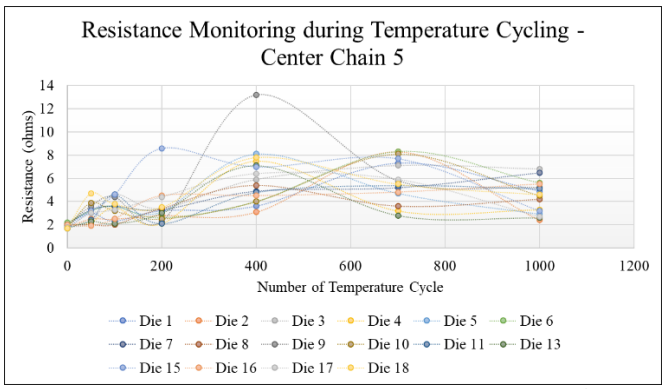

Figure 12: Resistance monitoring through temperature cycling of center Chain #5. These chains exhibited the lowest initial resistance pre-cycling.

Table II shows the resistance change through 1000 cycles. Resistance increased for all three chains, with Chain 5 (center) having the largest increase. All samples initially exhibited a lower resistance for Chain 5 than any of the outer chains, thereby suggesting that thermal cycling normalized the resistance values of all chains. Post-temperature cycling resistance values are shown in Fig. 13 for all die, with resistance values typically ranging from 3-10 Ω.

Table III: Resistance change through 1000 temperature cycles for the center (Chain #5) and two corner chains (Chains #7 and #9).

Sample	Chain 5	Chain 7	Chain 9
Die 1	2.9	2.1	1.1
Die 2	0.6	3.0	4.2
Die 3	5.0	3.9	2.7
Die 4	1.3	0.1	0.7
Die 5	0.9	3.0	3.8
Die 6	3.4	0.6	0.2
Die 7	4.5	0.4	1.8
Die 8	2.2	0.5	2.9
Die 9	3.2	0.8	0.3
Die 10	2.8	1.1	3.7
Die 11	3.3	1.2	0.5
Die 13	0.9	1.9	1.4
Die 15	1.5	0.6	2.5
Die 16	3.5	1.9	1.1
Die 17	0.9	0.9	1.3
Die 18	2.9	0.9	1.3
Ave	**2.5**	**1.4**	**1.8**

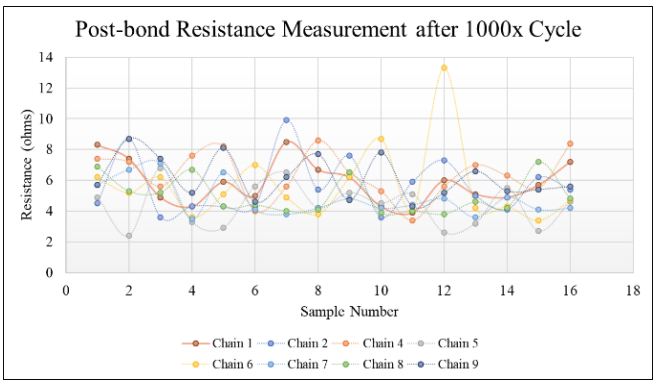

Figure 6: Post-bond resistance measurements for all samples and chains after 1000 temperature cycles.

A representative cross-section of the Cu-to-Cu bonded interconnects post-temperature cycling is shown in Fig. 14. A slight seam was observed after the cycling, which possibly limits the reliability of the parts beyond 1000 cycles; however no major electrical degradation was noted. In the next section, we highlight future steps to examine this degradation.

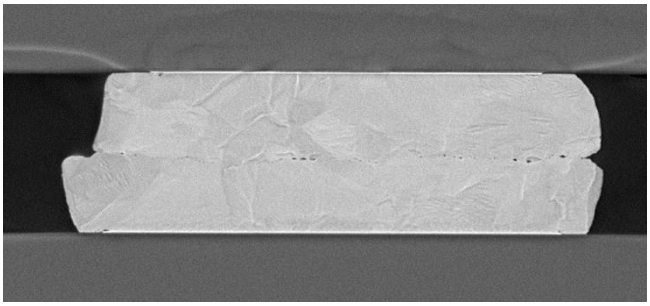

Figure 14: Cross-section of joint post-temperature cycling for 1000 cycles, showing formation of some interface seams.

V. Next Steps

Next steps to examine the interface quality and reliability include characterizing the grain structure of the copper pads. Grain structure has been known to influence bonding characteristics [7]. Therefore, it is critical to analyze how grain structure of copper affects the bonding process described here without a separate annealing process. Additionally, there may be a need for underfill or non-conductive material to protect the joints for bonding in different applications. Investigating a pre-applied underfill method described in [8] may provide improvements in reliability. Lastly, bonding time was not considered in this paper, but continued investigations should determine how bond strength varies with different bonding times. These parameters are worth exploring to further develop this bonding process.

VI. Conclusion

Data presented in this paper shows that direct Cu-to-Cu bonding without annealing is a viable process. Cross-section analysis and die shear force indicate good interconnect alignment, joint formation, and bond strength. However, the temperature cycling data shows slight degradation of the joints during the temperature cycling. So further work is likely required before the process is ready for production. Despite this, this demonstration shows that the advantages of a solderless copper to copper bonding process can be leveraged without the needs of additional processing time brought forth through the anneal process.

Acknowledgment

The successful completion of this work was made possible by the dedicated collaboration between multiple teams at the Northrop Grumman Corporation. This includes the Test team in Apopka Florida, the Emerging Capabilities Manufacturing Engineering (ECME) department in Baltimore the Reliability Analysis Lab (RAL) of the Advanced Technology Laboratory (ATL) in Baltimore and many others.

References

[1] Bumps vs. Hybrid Bonding for Advanced Packaging, “Bumps Vs. Hybrid Bonding For Advanced Packaging (semiengineering.com)”.

[2] N. Shakoorzadeh, S. C. Jangam, K. Rahim, P. Ambhore, H. Chien, A. N. Hanna, S. Iyer, ” Reliability Studies of Silicon Interconnect Fabric,” 2019 IEEE 69th Electronic Components and Technology Conference (ECTC).

[3] J.W. Huang, K.C. Shie, H.C. Liu, Y.J. Li1, H.Y. Cheng, and C. Chen, “Copper- to-copper direct bonding using different (111) surface ratios of nanotwinned copper films,” ICEP 2019 Proceedings.

[4] H. Moriceau, F. Rieutord, F. Fournel, L. DiCioccio, C. Moulet, L. Libralesso, P. Gueguen, R. Taibi, C. Deguet, “Low temperature direct bonding: An attractive technique for heterostructures build-up,” Microelectron. Reliab. 52 (2012), pp. 331–341. doi:10.1016 j.microrel.2011.08.004, 2011.

[5] W. Yang, et al. “Study of Cu film surface treatment using formic acid vapor/solution for low temperature bonding.” Journal of The Electrochemical Society 165.4 (2017): H3080.

[6] “What Are Taguchi Designs?” NIST/SEMATECH e-Handbook of Statistical Methods, July 2003, doi.org/10.18434/M32189

[7] I. Panchenko, L. Wenzel, M. Mueller, C. Rudolph, A. Hanisch and J. M. Wolf, “Microstructure Development of Cu/SiO_2 Hybrid Bond I.nterconnects After Reliability Tests," in IEEE Transactions on Components, Packaging and Manufacturing Technology, vol. 12, no. 3, pp. 410-421, March 2022, doi: 10.1109/TCPMT.2022.3149788.

[8] N. Lay, N. DiNapoli, K. Rahim, PhD., S. Razmyar, PhD., and M. Holliday. 2023. “Pre-Applied Underfill Technique for Fine-Pitch Cu Pillar 3D Die Stacking to Enable 2.5/3D Advanced Packaging.” IMAPSource Proceedings 2022 (Issue 1): 000273–79.